

# Tip-Enhanced Raman Scattering of *Bacillus subtilis* spores

G. Rusciano<sup>\*a</sup>, G. Zito<sup>a</sup>, G. Pesce<sup>a</sup>, A. Sasso<sup>a</sup>, R. Isticato<sup>b</sup>, E. Ricca<sup>b</sup>

<sup>a</sup> Dept. of Physics, University of Naples Federico II, via Cintia, 80126-I Naples, Italy;

<sup>b</sup> Dept. of Biology, University of Naples Federico II, via Cintia, 80126-I Naples.

## ABSTRACT

Understanding of the complex interactions of molecules at biological interfaces is a fundamental issue in biochemistry, biotechnology as well as biomedicine. A plethora of biological processes are ruled by the molecular texture of cellular membrane: cellular communications, drug transportations and cellular recognition are just a few examples of such chemically-mediated processes. Tip-Enhanced Raman Scattering (TERS) is a novel, Raman-based technique which is ideally suited for this purpose. TERS relies on the combination of scanning probe microscopy and Raman spectroscopy. The basic idea is the use of a metallated tip as a sort of optical nano-antenna, which gives place to SERS effect close to the tip end. Herein, we present the application of TERS to analyze the surface of *Bacillus subtilis* spores. The choice of this biological systems is related to the fact that a number of reasons support the use of spores as a mucosal delivery system. The remarkable and well-documented resistance of spores to various environmental and toxic effects make them clear potentials as a novel, *surface-display* system. Our experimental outcomes demonstrate that TERS is able to provide a nano-scale chemical imaging of spore surface. Moreover, we demonstrate that TERS allows differentiation between wild-type spore and genetically modified strains. These results hold promise for the characterization and optimization of spore surface for drug-delivery applications.

**Keywords:** Tip-Enhanced Raman Scattering (TERS), bacterial spores, drug-delivery, surface-display systems.

## 1. INTRODUCTION

The development of newly conceived tools for drug-delivery applications is certainly an emerging research field, as witnessed by the growth of research and applications in recent years. Surface-display systems - living microorganisms displaying recombinant proteins and peptides on their surface - represent a significant step forward. In particular, bacterial spores displaying heterologous antigens adsorbed on their surface have shown clear potentials as a novel surface display system for the delivery of bio-therapeutic molecules to human mucosal surfaces [1]. Importantly, the safety record of several endospore-forming species, makes spores of those species ideal candidates as vehicles to deliver molecules to mucosal surfaces. Adsorbed molecules are stabilized and protected by the interaction with the spore, suggesting that this system could reduce the rapid degradation of the antigen, often observed with other delivery systems and identified as a major drawback of mucosal vaccines. Although the molecular details of spore adsorption have not been fully addressed, spores have shown clear potentials as a novel surface display systems that, being non-recombinant and based on a host with a remarkable safety record, appear particularly well suited for the delivery of bio-therapeutic molecules to human mucosal surfaces. A complete understanding of the physicochemical properties of the spore surface is then essential for a rational design of the molecules to be displayed and to optimize the efficiency of the non-recombinant display system. Optical methods are ideally suited for the analysis of bio-interfaces. In particular, Raman spectroscopy has recently emerged as a formidable alternative to fluorescence, as demonstrated by the increasing number of applications in many fields of life sciences [2-4]. The "fingerprint" character of this spectroscopic technique has provided access to the biochemical composition of many bio-systems, and its evolution under the application of external stimuli. Furthermore, the traditional drawback of Raman spectroscopy, namely its relatively low cross-section compared with fluorescence-based spectroscopic techniques, has been recently overcome by the discovery of the enhancement of the Raman spectrum when Localized Surface Plasmonic Resonances (LSPRs) excited by the Raman probe. This phenomenon is called Surface-Enhanced Raman Scattering (SERS) and, since its discovery, its use as analytical technique has grown exponentially [5-11]. SERS enhancement can reach up to 12 orders of magnitudes providing single-molecule sensitivity [9] and nanoscale spatial localization ("hot spot") that allows sub-diffraction resolution. Very recently, a new research field has emerged that conjugates the high sensitivity of SERS with the

\*giulia.rusciano@unina.it phone +39 081676273

nanometre scale resolution of scanning probe microscopes and is termed Tip-Enhanced Raman Scattering (TERS) [12]. TERS relies on the combination of near-field scanning probe microscopy and enhanced Raman spectroscopy. In TERS, in fact, a metallated tip is used as a sort of optical nano-antenna that gives place to the SERS amplification only at the tip apex of the scanning probe, which in turn allows near field, sub-diffraction resolution. TERS allows obtaining simultaneously topographic and chemical information of the analysed surface region, which constitutes an important step for surface analysis in its broadest sense. These features make TERS a unique tool to directly localize and identify proteins and their conformation in a complex (e.g., native) environment. In particular, it proved to be an excellent technique for detailed investigations of biomolecules that are adsorbed, layered, or assembled on a large variety of surfaces and interfaces [13-16]. Herein, we present the results regarding the TERS characterization of the surface of *B. subtilis* spores (the coat) owing to two different strains. Current knowledge of spore coat is in fact based only on Western blot analysis of solubilized extracts from the spore coat, a technique which obviously implies a complete loss of information on the chemicals' distribution of the spore surface, and, more importantly, on the arrangement of the chemical functionalities. On the contrary, information on the chemical distribution as provided by TERS could represent a significant step toward rational designing of the coat molecules to be displayed and optimization of the non-recombinant display system.

## 2. METHODOLOGY

### Experimental set-up

The TERS setup used for this investigation is described in ref. [13]. Briefly, it is based on the WITec Alpha 300 system and consists in an AFM system mounted on an inverted Raman microscope (Fig. 1). A linearly polarized laser at 532 nm was used as Raman excitation source. A dry, 60X objective (PlanApo, Olympus, NA 0.8) was used to focus the excitation laser on the sample. Sample scanning was performed by a closed-loop XY piezo scanning stage (P-734, Physik Instrumente, Germany), allowing sample positioning with an accuracy of 1 nm.

TERS tips, provided by Next-Tip S.L., consisted of commercial AFM tips with elastic constant of 2.8 N/m and resonance frequency at ca. 75 kHz, on which ~ 14 nm gold nanoparticles (Au-NPs) were deposited upon ultra-high vacuum conditions. For the analysis, 50  $\mu$ l of a water suspension of mature PY79 wild type spores at a concentration of  $10^5$  spore/ml were pipetted on a clean glass coverslip and left to dry at ambient conditions for 24 hours.

In order to prevent damage of the relatively soft spore surface caused by the interaction of the tip, AFM analysis was performed in AC mode. Moreover, sample photodamage was avoided by limiting the power impinging on the sample to a few tens of  $\mu$ W. Before TERS investigation, preliminary AFM images of the spore were acquired in order to select the points to be probed. Then, the laser probe was switched on and tip engagement was optimized upon laser irradiation. Therefore, TERS signal was maximized by matching the laser focus with the tip apex by means of a piezo-driver controlling the focusing objective. In particular, the optimum Raman beam focus in the x-y plane (see Fig. 1) was searched by monitoring the Raman signal from the bulk Si of the tip.

### *B. subtilis* spores

*B. subtilis* is, among the spore-forming bacilli, the best characterized species and is an important model system to study complex biological phenomena, like differentiation, cell-cell communication and biogenesis of complex cellular structures. Its innermost part, called the core, contains dehydrated cytoplasm with proteins, stable RNAs and DNA. This

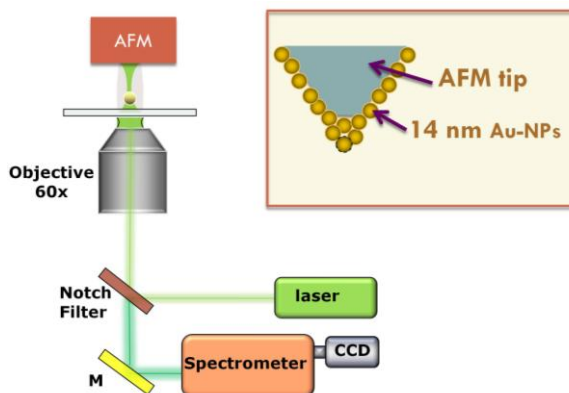


Figure 1. A sketch of the experimental set-up employed for this investigation. The inset shows a sketch of the TERS tip used in this work.

dehydrated physical state of the core plays an important role in spore dormancy and heat resistance and is due to the presence of spore-specific compound pyridine-2,6-dicarboxylic acid (dipicolinic acid or DPA).

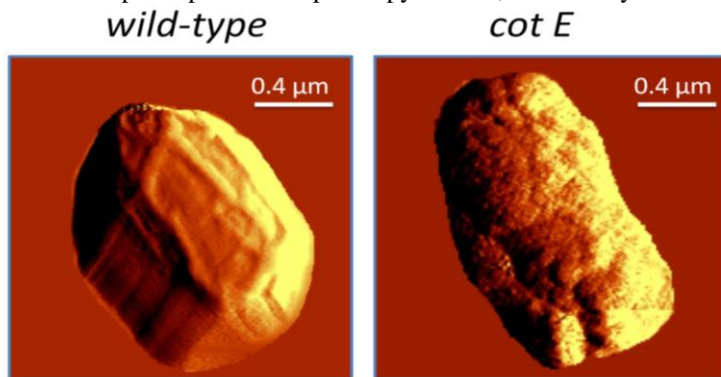


Figure 2. AFM-amplitude images of *B. subtilis* spores. The left image corresponds to a *wild type* spore, while the right image correspond to a genetically modified spore.

The spore core is surrounded by two main layers: the cortex, a modified peptidoglycan, and the coat, a multilayered proteinaceous structure. The coat represents the outermost layer of the spore and protects the spore from toxic chemicals and lytic enzymes. At the electron microscope, the coat appears composed by three different sublayers: a lightly staining lamellar inner coat, a darkly staining coarsely layered outer coat and the crust, a most recently observed layer. The coat is composed by more than 70 different proteins, about 10% of the spore dry weight, and glycans. While the protein components have been identified and widely studied, carbohydrates associated to the spore surface have not been characterized in details.

### 3. RESULTS AND DISCUSSION

In this study, we analyzed two different *B. subtilis* strains: the wild type and a mutant, named *cotE*, lacking of a morphogenic protein (CotE). As reported previously [17,18], this protein forms a ring-like structure which surrounds the forming spore and drives the formation of the outermost layers, the outer coat and the recently identified crust. Strain mutant in this protein are lacking of the outer coat and the crust layers.

As mentioned before, the first step of our analysis was the acquisition of AFM maps of spores. For this preliminary analysis, uncoated silicon probes (Nanoworld, Arrow<sup>TM</sup> FM) of resonant frequency of 75 kHz were used. Figure 2 shows the height images captured for wild type and *cotE* spores. They were obtained with a scan step of 10 nm and a scan rate of 200 points/s. The driving frequency was decreased with respect to the resonant peak of the cantilever to have 90% of the peak amplitude as driving amplitude.

The AFM images of Fig. 2 are presented without any digital manipulation. Clearly, both images exhibit imaging artefacts typically occurring in height objects [19], consisting in bright zones or dark shadows at the spore border, due to the interaction of the edge of the tip with the spore. However, a clear difference can be seen between the two analysed strains. In particular, wild type spores morphology clearly exhibits surface ridges, mainly extending along the main spore axis. As reported in ref. [20], the ridges function is probably connected to the spore capability to accommodate volume changes occurring during spore core dehydration and re-hydration. The presence of clearly identifiable surface structures is quite less pronounced in *cotE* spores, as results of the lack of the outermost layer induced by the genetic mutation. In both spore strains, a more complex pattern with respect to the bare topographic image can be seen in the AFM-phase images. In Figure 3 we report the spontaneous Raman scattering signal of wild-type (trace a) and *cotE* (trace b). They were obtained by using a laser power of 0.5 mW and an integration type of 20 s. The relative high integration time used for this acquisition is due to the relatively low Raman activity of spores, reported previously [18]. The two spectra appear quite similar being, in both cases, essentially due the calcium dipicolinate (CaDPA) contained in the inner shell of both spores. Instead, the very thin more external layer (the coat) provide no significant contributions to this spectra. By comparing the intensity of selected peaks in trace a and c, it is possible to estimate the enhancement factor provided by the plasmonic tip. In particular, by choosing the peak at  $1001\text{ cm}^{-1}$ , not visible in the Raman spectrum of CaDPA and likely ascribable to proteins present on the external layer, it is reasonable to use the following relation, strictly valid only for thin samples [21]:

$$EF=OC \cdot (A_{FF}/A_{NF}) \quad (1)$$

The first factor in equation 1 is normally referred to as Optical Contrast and provided by the ratio  $OC=(I_{tip-in}-I_{tip-out})/I_{tip-out}$  where  $I_{tip-in}$  and  $I_{tip-out}$  correspond to the signal acquired with the tip engaged or disengaged, respectively. The second factor in Eq. (1) takes into account that the investigated area in far-field ( $A_{FF}$ ) is much larger than the area that is illuminated by the tip in near-field ( $A_{NF}$ ).

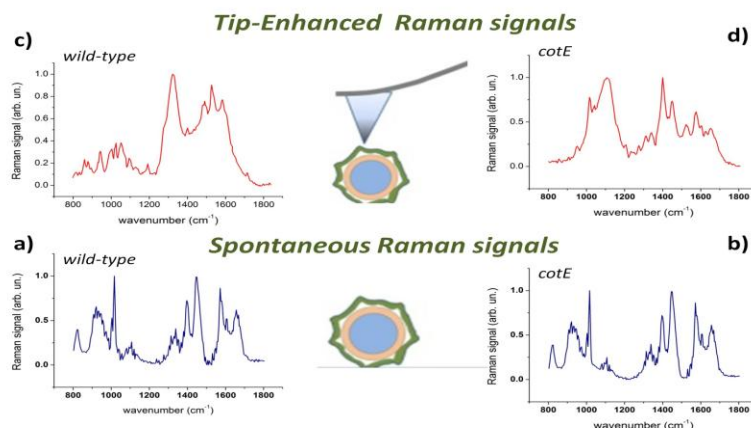


Figure 3. Spontaneous Raman (a,b) and TERS signals (c,d) of *B. subtilis* spores, as indicated in the figure labels.

Spectral assignment	
Raman shift ( $cm^{-1}$ )	Assignment
830	$\nu_{as}(O-P-O), \nu_{ring}(C-C)$ (Tyr)
930	$\delta(C-C-O)$
1001	$\nu(C-C)$ (aromatic ring) (Phe)
1030	$\nu(C-C)$
1091	$\nu_s(PO_2)$ , Glycosidic ring breathing
1128	Glycosidic ring breathing
1205	$\nu_s(PO_2)$ , Amide III (Tyr, Phe)
1338	Amide II (Trp)
1373	$\nu_s(COO^-), \delta(CH_3)$
1445	$\delta(CH_2), \delta(CH_3)$
1546	Amide II
1574	Amide II (Phe, Trp)

Table 1. Tentative assignment of the main TERS bands observed in this work.

By assuming  $A_{FF}=4.3 \cdot 10^5 \text{ nm}^2$  and  $A_{NF}=310 \text{ nm}^2$  (corresponding to a circle with a 20 nm diameter), it is possible to obtain  $EF=7.6 \cdot 10^4$ , in line with typical values reported in TERS investigations. It is worth noting TERS spectra exhibit large variation from point to point, suggestive that the spatial resolution is even better than the scan step. Intriguingly, spectra are stable and reproducible, as confirmed by the similarity of successive acquisitions in the same point (data not shown). In the TERS spectra of Fig. 3 many characteristic peaks are visible. A complete assignment of these features is reported in Table 1. In particular, bands typically related to amino acids were clearly distinguishable, such as the band around  $830 \text{ cm}^{-1}$ , ascribable to C-C symmetric ring stretching of Tyrosine, the band at  $1001 \text{ cm}^{-1}$ , owing to symmetric ring breathing in Phenylalanine, as well as bands around 1546 and  $1574 \text{ cm}^{-1}$ , due to Tyrosine and Tryptophan ring vibration, respectively. We also ascribed numerous bands frequently observed in our TERS spectra to carbohydrates and/or glycans of glycoproteins. In particular, bands around 930, 1030, 1091, 1128, and  $1205 \text{ cm}^{-1}$  can be attributed to C-C, C-O, C-C, C-O-H and C-O-C stretching, respectively. Instead, as found in many other TERS investigations, features in the spectral range between 1640 and  $1690 \text{ cm}^{-1}$  were only occasionally visible [22].

#### 4. CONCLUSIONS

In conclusion, we have demonstrated that TERS analysis is a unique, powerful tool to get insight on the presence and the arrangement of chemical functionalities on the surface of *B. Subtilis* spores owing to different

strains. This information constitutes a first crucial step for the development of spore-based surface-display systems and drug delivery applications.

#### ACKNOWLEDGEMENTS

GZ acknowledges a postdoctoral fellowship under grant number *FIRB 2012-RBFR12WAPY* supported by Italian Ministry for Education, University and Research (MIUR). This research was supported in part by *Programma STAR* of

## REFERENCES

- [1] Isticato R., Sirec T., Treppiccione L., Maurano F., De Felice M., Rossi M., Ricca E. "Non-recombinant display of the B subunit of the heat labile toxin of Escherichia coli on wild type and mutant spores of Bacillus subtilis", *Microb Cell Fact*, 12, 98-108 (2013).
- [2] Stewart S., Priore R.J., Nelson M.P., Treadoet P.J. "Raman Imaging" *An. Rev. Anal. Chem.*, 5, 337-360 (2012).
- [3] Rusciano G. "Experimental analysis of Hb oxy-deoxy transition in single optically stretched red-blood cells" *Physica Medica: European Journal of Medical Physics* 26 233-239 (2010).
- [4] Rusciano G., De Luca A.C., Pesce G., Sasso A. "Enhancing Raman Tweezers by phase-sensitive detection" *Anal. Chem.* 79 3708-3715 (2007).
- [5] Fleischmann M., Hendra P.J., McQuillanet A.J. "Raman Spectra of Pyridine Adsorbed at a Silver Electrode" *Chem. Phys. Lett.*, vol. 26, 163-166 (1974).
- [6] Nie S., Emory S.R. "Probing single molecules and single nanoparticles by surface-enhanced Raman scattering" *Science*, 275, 1102-1106 (1997).
- [7] Minutolo P., Rusciano G., Sgro L.A., Pesce G., Sasso A., D'Anna A. "Surface enhanced Raman spectroscopy (SERS) of particles produced in premixed flame across soot threshold" *Proc. Comb. Inst.* 33, 649-657 (2011).
- [8] Rusciano G., De Luca A.C., Pesce G., Sasso A. "On the interaction of nano-sized organic carbon particles with model lipid membranes" *Carbon* 47 2950-2957 (2009).
- [9] Sgro, L. A., Sementa, P., Vaglieco, B.M., Rusciano, G., D'Anna, A., Minutolo P, "Investigating the origin of nuclei particles in GDI engine exhausts" - *Combustion and Flame*" 159 (4) 1687-1692 (2012).
- [10] De Rosa, C., et al., "Toward hyperuniform disordered plasmonic nanostructures for reproducible surface-enhanced Raman spectroscopy" *Phys. Chem. Chem. Phys.*, 17, 8061-8069 (2015).
- [11] Zito G., et al., "Surface-enhanced Raman imaging of cell membrane by a highly homogeneous and isotropic silver nanostructure" *Nanoscale*, 7, 8593-8606 (2015).
- [12] Inouye Y., et al. "Near-field scanning optical microscope using a metallized cantilever tip for nanospectroscopy" *Proc. of SPIE*, 3791, 40-48 (2003).
- [13] Rusciano G., Zito G., Isticato R., Sirec T., Ricca E., Bailo E, Sasso, A. "Nanoscale Chemical Imaging of Bacillus subtilis Spores by Combining Tip-Enhanced Raman Scattering and Advanced Statistical Tools" *ACS NANO*, 8, 12300-12309 (2014).
- [14] Bailo E., Deckert V. "Tip-Enhanced Raman Scattering" *Chem. Soc. Rev.*, 37, 921-930 (2008).
- [15] Stadler J., Schmid T., Zenobi R. "Nanoscale Chemical Imaging Using Top-Illumination Tip-Enhanced Raman Spectroscopy" *Nano Lett.*, 10, 4514-4520 (2010).
- [16] Nakata, A.; Nomoto, T.; Toyota, T.; Fujinami, M. Tip-Enhanced Raman Spectroscopy of Lipid Bilayers in Water With an Alumina- and Silver-Coated Tungsten Tip. *Anal.Sci.*, 29, 865-869 (2013).
- [17] Zheng L., Donovan W.P., Fitz-James P.C., Losick R. "Gene encoding a morphogenic protein required in the assembly of the outer coat of the Bacillus subtilis endospore" *Genes Develop.*, 2: 1047-1054 (1988).
- [18] Isticato R., Sirec T., Giglio R., Baccigalupi L., Rusciano G., Pesce G., Zito G., Sasso A., De Felice M., Ricca E. "Flexibility of the programme of spore coat formation in Bacillus subtilis: bypass of CotE requirement by over-production of CotH" - *PLoS ONE* 8 e74949 (2013).
- [19] Velegol S.B., Pardi S., Li X., Velegol D., Logan B.E. "AFM imaging artefacts due to bacterial cell height and AFM Tip Geometry", *Langumir*, 19, 851-857 (2003).
- [20] Sahin O., Yong E.H.; Driks, A.; Mahadevan, L." Physical Basis for the Adaptive Flexibility of Bacillus Spore Coats". *J. R. Soc. Interface*, 9, 3156-3160 (2012).
- [21] Schmid T., Messmer A., Yeo B.S., Zhang W.H., Zenobi R. "Towards Chemical Analysis of Nanostructures in Biofilms II: Tip-Enhanced Raman Spectroscopy of Alginates." *Anal. Bioanal. Chem.*, 391, 1907-1916 (2008).
- [22] Blum C., Opilik L., Metanis N., Weidmann S., Zenobi, R "Missing Amide I Mode in Tip-Enhanced Raman Spectra of Proteins?. *J. Phys. Chem. C*, 116, 23061-23066 (2012).